tvst

Article

Comparison of Rates of Progression of Macular OCT Measures in Glaucoma

Alessandro Rabiolo[1,2], Vahid Mohammadzadeh[1], Nima Fatehi[1], Esteban Morales[1], Anne L. Coleman[1], Simon K. Law[1], Joseph Caprioli[1], and Kouros Nouri-Mahdavi[1]

[1] Stein Eye Institute, David Geffen School of Medicine, University of California Los Angeles, Los Angeles, CA, USA
[2] Department of Ophthalmology, University Vita-Salute, IRCCS San Raffaele, Milan, Italy

Correspondence: Kouros Nouri-Mahdavi, Stein Eye Institute, David Geffen School of Medicine, University of California Los Angeles, Los Angeles, CA 90095, USA. e-mail: Nouri-Mahdavi@jsei.ucla.edu.

Received: December 10, 2019
Accepted: April 5, 2020
Published: June 30, 2020

Keywords: full macular thickness; ganglion cell complex; ganglion cell/inner plexiform layer; ganglion cell layer; macular sectors; OCT, progression; rates of change

Citation: Rabiolo A, Mohammadzadeh V, Fatehi N, Morales E, Coleman AL, Law SK, Caprioli J, Nouri-Mahdavi K. Comparison of rates of progression of macular OCT measures in glaucoma. Trans Vis Sci Tech. 2020;9(7):50, https://doi.org/10.1167/tvst.9.7.50

Purpose: The purpose of this study was to compare rates of change of various macular thickness measures and evaluate the influence of baseline damage on macular rates of change.

Methods: One hundred twelve eyes (112 patients) with $\geq$ 2 years of follow-up and $\geq$ 5 macular optical coherence tomography (OCT) images and 10-2 visual field (VF) tests were included. OCT measures of interests were full macular thickness (FMT), ganglion cell complex (GCC), ganglion cell/inner plexiform layer (GCIPL), ganglion cell layer (GCL), and outer retinal layer (ORL) thickness in 3° $\times$ 3° superpixels. Rates of change were estimated with linear regression and normalized by dividing rates by the average normative superpixel thickness. We compared rates of change and proportion of significantly worsening superpixels (detection rate) and improving superpixels (false discovery rate [FDR]) among macular measures as a function of baseline thickness and 10-2 VF status.

Results: Median (interquartile range [IQR]) baseline VF mean deviation, follow-up time, and number of VFs/OCTs were −7.6 dB (−11.8 to −3.8 dB), 4.5 years (4.0–5.0 years), and 9 (8–10), respectively. Normalized FMT and GCC rates of change were faster and detection rates were higher than GCIPL and GCL ($P < 0.001$), but FMT had lower FDR than GCC ($P = 0.02$); faster FMT rates were partially explained by ORL rates of change. GCC detection rates were less likely than GCIPL and GCL rates to decrease with diminishing baseline thickness or worse VF damage. In eyes with 10-2 VF worsening, GCC and GCL demonstrated the fastest rates of change.

Conclusions: GCC measurements are most likely to detect structural worsening along the spectrum of glaucoma severity. Although FMT rates of change are least influenced by baseline thickness, they partially reflect likely age-related ORL changes.

Translational Relevance: GCC thickness measurements seem to be the optimal macular outcome measure for detection of glaucoma deterioration.

Introduction

Timely identification of disease progression in moderately to severely advanced glaucoma is a critical but challenging task because both functional and structural measures become less informative than in early disease.[1] Although visual field (VF) testing remains the main method for detection of glaucoma progression, higher long-term fluctuation with progressing glaucomatous damage is a major confounding factor for identifying disease deterioration, particularly at advanced stages of the disease.[2] Detection of progression with optic disc photographs has poor interobserver reproducibility and may be of uncertain utility in advanced disease where the neuroretinal rim is severely thinned.[3,4] Spectral-domain optical coherence tomography (SD-OCT) is a commonly used technique for measuring structural progression. The peripapillary retinal nerve fiber layer (RNFL) thickness reaches its measurement floor when the mean deviation or sectoral total deviation, defined as the average of the total

Copyright 2020 The Authors

This work is licensed under a Creative Commons Attribution-NonCommercial-NoDerivatives 4.0 International License.

deviation values within a sector, reaches about −8 to −10 dB.[5,6] Recent studies have shown that macular measures tend to reach their measurement floor later than RNFL and may be able to detect change in later stages of the disease.[7–10]

Measurement of the ganglion cell layer (GCL) has been considered the ultimate outcome measure to gauge and monitor glaucomatous damage in the macula, but the utility of measuring the GCL proper remains questionable with current optical coherence tomography (OCT) technology.[11] We have previously shown that thickness variability is low and uniform for all macular outcome measures and, therefore, the relative measurement variability is inversely related to the average thickness of a given macular outcome measure.[12] The same study found that thickness variability increased at very low thickness levels for GCL and ganglion cell/inner plexiform layer (GCIPL), likely due to more challenging segmentation with diminishing thickness and density gradients. Segmentation errors are more frequent with thinner retinal nerve fiber layer, which may confound the identification of structural progression.[13,14] We hypothesized that full macular thickness (FMT) or ganglion cell complex (GCC) thickness measurements would perform better than GCIPL or GCL measures to detect glaucoma progression in eyes with moderately to severely advanced glaucoma, given the lower measurement noise and more reliable segmentation.

The outer half of the retina beyond the inner plexiform layer (outer retinal layers [ORLs]) is not affected by glaucoma, and ORL measurements do not distinguish between healthy and diseased eyes or identify glaucomatous progression.[15–18] A cross-sectional study estimated that the entire retina thinned out at a rate of −0.24 µm/year and that the outer nuclear layer had the fastest rate among the individual layers (−0.1 µm/year).[19] Although glaucoma leads to thinning of the inner retinal layers, ORL thinning is not expected to occur in glaucoma.[15–18]

The goals of the current study are: (1) to compare the magnitude of rates of change at the level of superpixels and empirically defined macular sectors for four macular outcome measures consisting of FMT, GCC, GCIPL, and GCL thickness and compare those to ORL rates of change; (2) to define empirical macular sectors based on correlation of structural rates of change; (3) to estimate the influence of baseline glaucoma damage on the performance of the above measures to detect progression; and (4) to compare structural rates of progression in stable and progressing eyes according to central VFs.

Methods

Study Sample

Eyes from the Advanced Glaucoma Progression Study (AGPS), an ongoing longitudinal study at the University of California Los Angeles (UCLA), with a minimum of five 10-2 VF and macular OCT images, ≥ 2 years of follow-up, and no other ocular pathology at baseline and during follow-up were recruited. The study adhered to the tenets of the Declaration of Helsinki, was approved by UCLA's Human Research Protection Program, and conformed to the Health Insurance Portability and Accountability Act (HIPAA) policies. All patients provided written informed consent at the time of enrollment in the study. The enrolled eyes met the following inclusion criteria: (i) clinical diagnosis of primary open-angle glaucoma, pseudoexfoliative glaucoma, pigmentary glaucoma, or primary angle-closure glaucoma; (ii) evidence of either central VF damage on 24-2 VFs, defined as two or more points within the central 10° with $P < 0.05$ on the pattern deviation plot or VF mean deviation (MD) worse than −6 dB. Exclusion criteria were: baseline age < 40 or > 80 years; best-corrected visual acuity < 20/50; refractive error exceeding 8 diopters (D) of sphere or 3 D of cylinder; and any significant retinal or neurological disease potentially affecting OCT measurements.

Imaging and VF Procedures

Macular imaging was carried out with the Posterior Pole Algorithm of Spectralis SD-OCT (Heidelberg Engineering, Heidelberg, Germany). The Posterior Pole algorithm acquires 30° × 25° volume scans of the macula (61 B-scans spaced approximately 120 µm) centered on the fovea. The software segments the central 24° × 24° of the measurement cube and presents data in an 8 × 8 array of 3° × 3° superpixels (Supplementary Fig. S1). Each B-scan was repeated 9 to 11 times to improve image quality. The following layers were included in the study: (i) FMT, which is limited by the inner limiting membrane (ILM) and the retinal pigment epithelium/Bruch's membrane complex, and includes all the retinal layers; (ii) GCC, delimited by the ILM and the inner plexiform layer (IPL)/inner nuclear layer (INL) boundary, and includes the macular retinal nerve fiber layer (mRNFL), GCL, and IPL; (iii) GCIPL, which is delimited by the mRNFL/GCL boundary and the IPL/INL boundary, and includes the GCL and the IPL; (iv) GCL, and (v) ORL, which extends from the outer border of the IPL

to the retinal pigment epithelium/Bruch's membrane complex.

Automated segmentation of individual retinal layers was performed with the Glaucoma Module Premium Edition software before data export. Images were reviewed for segmentation errors and image artifacts. Any obvious segmentation errors were manually corrected with the SD-OCT device's built-in software. If more than two B-scans within the central 24° of any individual volume scan were of inadequate quality or showed poor segmentation, that session was excluded from analyses. A low-quality B-scan image was defined as quality factor < 15, presence of more than 10% missing data or inadequate segmentation, or any artifacts such as mirror artifacts.

Central 10-2 VFs with false positive rates of 15% or less were included. Perimetric progression was evaluated with pointwise linear regression (PLR) of threshold sensitivities over time. Each test location was described as deteriorating (rate of change ≤ -1 dB/year at $P < 0.01$), improving (rate of change ≥ 1 dB/year at $P < 0.01$), or otherwise stable. A VF series was defined as progressing if there were more than or equal to three deteriorating test locations after accounting for improving locations. Because VF progression greatly depends on the method used to define progression,[20,21] we also repeated all the analyses using another pointwise PLR criterion (≥ 4 deteriorating test locations with a rate of change ≤ -1 dB/year at $P < 0.05$) as well as the regression of the global index MD against time (progression defined as negative rate of change at $P < 0.05$).

Statistical Analyses

Rates of change were estimated with univariate linear regression analysis of thickness against time. A separate regression was carried out for each eye's superpixels and sectors, and for each macular outcome measure (FMT, GCC, GCIPL, GCL, and ORL). As various macular measures have different average thicknesses, raw rates of progression are not directly comparable; we normalized the rates of change by dividing them by the average thickness at corresponding superpixels/sectors using the normative database provided by Heidelberg Engineering.

We graphically compared the mean and SD of raw rates of change at 64 superpixels for various macular outcome measures. Given the nongaussian distribution of rates of change, we compared normalized rates of change with nonparametric tests. As there is no true external standard to which structural rates of change can be compared, we compared detection rates and false discovery rates (FDRs) among macular measures. The former was described as the percentage of superpixels (or sectors) demonstrating a "significant" negative rate of change defined as a negative rate with a P value < 0.05. Conversely, FDRs consisted of the percentage of superpixels (or sectors) showing a positive rate with corresponding $P < 0.05$. The detection rates and FDRs were compared among the different measures of interest with a logistic mixed model, where the detection rate or the FDR were the outcome variables, the macular measure of interest the fixed factor, and the eye ID the random effect to account for within-eye correlations due to the inclusion of multiple observations (various SPs) from the same eye. Pairwise differences among the measures of interest were tested with Tukey test.

Cluster analysis of raw rates of change at superpixels for FMT, GCC, GCIPL, and GCL was used to define macular sectors. To adjust for the different normal thickness among the various SPs and measures of interest, we carried out partial correlation analyses for the raw rates of change of all pairs of SPs adjusted for their pooled normal thickness. Pairwise partial correlations were performed between SPs belonging to the same measure of interest (i.e. different outcomes were not mixed). The dendrogram from cluster analysis was examined, and superpixels whose raw rates of change demonstrated correlation above an optimal threshold were combined into a single sector. The optimal number of clusters was chosen by means of an elbow plot. The magnitude of the rates of change within sectors and sectoral detection rates and FDR were compared among macular layers. We also compared rates of change at superpixels and sectors and detection rates and FDR in stable and progressing eyes based on 10-2 VF progression with linear mixed and logistic mixed models, respectively. In all the models, the eye ID was included as the random effect to account for within-eye correlation. The same analyses were repeated including only the central 24 superpixels.[10]

We divided baseline thickness measurements at superpixels into 10 deciles for each macular outcome measure and compared the rates of change and the proportion of worsening and improving rates of change for all these measures across the range of thickness measurements at baseline. We also compared the normalized rates of change, detection rates, and FDRs of various macular measures as a function of the baseline total deviation (TD) values at corresponding 10-2 VF locations. Baseline 10-2 VF TD values were flipped vertically and matched to individual macular superpixels after correcting for the retinal ganglion cell displacement (Supplementary Fig. S1).[22,23] Some superpixels did not have corresponding test locations

Table 1. Detection and False Discovery Rates for Individual Superpixels for Various Macular Measures

Macular Measure	Region of Interests	Detection Rate	False Discovery Rate
FMT	Superpixels	26.0%	3.5%
	Sectors	31.4%	2.6%
GCC	Superpixels	15.3%	4.5%
	Sectors	23.8%	4.1%
GCIPL	Superpixels	10.6%	4.3%
	Sectors	16.7%	3.9%
GCL	Superpixels	8.3%	3.9%
	Sectors	13.1%	3.0%
ORL	Superpixels	14.7%	3.0%
	Sectors	18.7%	3.1%

FMT, full macular thickness; GCC, ganglion cell complex; GCIPL, ganglion cell/inner plexiform layers; GCL, ganglion cell layer; ORL, outer retinal layers.

Detection rate was described as the percentage of superpixels demonstrating a negative slope (rate of change) with a *P* value of < 0.05. Conversely, the false discovery rate was defined as the percentage of superpixels demonstrating a positive slope (rate of change) along with a *P* value < 0.05.

and were excluded from this analysis; eventually 40 superpixels were included. In case more than one VF test location matched the same superpixel, TD values were averaged to obtain a single TD value. Total deviation values were categorized in three bins according to the severity of pointwise damage at baseline: > -6 dB, between -6 dB and -12 dB, and worse than -12 dB. Differences in continuous (i.e. normalized rates of change) and dichotomous (i.e. detection rates, FDRs) variables as a function of the baseline thickness and VF TD values were tested with linear and logistic mixed models, respectively. In all the models, the eye ID was used as the random effect to account for within-eye correlations. Pairwise differences among the measures of interest, baseline decile thickness, and baseline VF TD values were investigated with Tukey test.

Results

One hundred twelve eyes of 112 patients with a median (interquartile range [IQR]) age of 68.1 years (62.7-74.0 years) were included in this study. Most patients were Caucasian ($n = 59$), followed by Asian ($n = 24$), African American ($n = 15$), and Hispanic ($n = 14$) ethnicities. The majority of patients had a diagnosis of primary open-angle glaucoma ($n = 100$), followed by primary angle-closure glaucoma ($n = 7$), pseudoexfoliative glaucoma ($n = 4$), and pigmentary glaucoma ($n = 1$). Median (IQR) baseline 10-2 VF mean deviation, follow-up time, and number of VFs/OCTs were -7.6 dB (-11.8 to -3.8 dB), 4.5 years (4.0-5.0 years), and 9 (8-10), respectively. Figure 1 demonstrates the average mean and SD of raw rates of change at individual superpixels across the macula. The raw rates of change increased as a function of the thickness of the macular measure in normal eyes, with FMT demonstrating the fastest change rates. Figure 2 illustrates the topography of raw rates of change. Except for ORL, the fastest changing superpixels were observed in the pericentral macular region. The most nasal column of superpixels was excluded from all subsequent analyses as they demonstrated the highest variability. Detection rates and FDR for pooled individual superpixels according to outcome measure are displayed in Table 1. The FMT had the highest detection rate, followed by GCC, ORL, GCIPL, and GCL; the difference in detection rates was significant ($P < 0.001$, Tukey test) for all the pairwise comparisons, except for GCC and ORL ($P = 0.84$, Tukey test). Among the measures of interests, ORL and FMT had the lowest FDR but were not statistically different from each other ($P = 0.53$, Tukey test). Outer retinal layers had a significantly lower FDR compared to all the other measures ($P < 0.001$, Tukey test), whereas the FDR for FMT was similar to those for GCIPL ($P = 0.07$, Tukey test) or GCL ($P = 0.68$, Tukey test) but was significantly lower compared to GCC ($P = 0.02$, Tukey test).

Results of cluster analysis for defining macular sectors are presented in Figure 3. As shown in Supplementary Figure S2, the 56 macular superpixels (after exclusion of 8 nasal superpixels) were categorized into 9 sectors using a clustering criterion of correlation

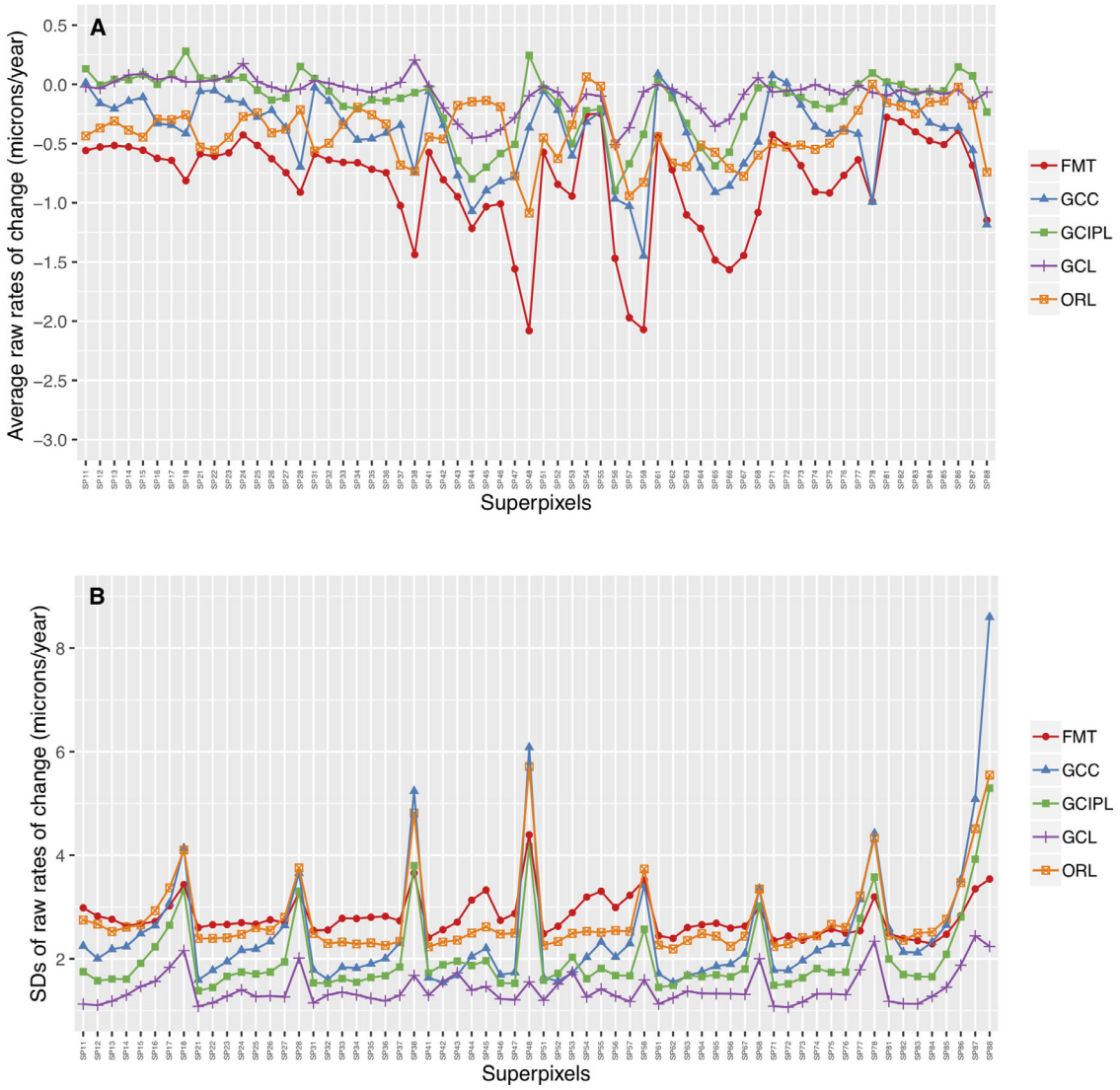

Figure 1. Average and standard deviation of the raw rates of change at individual superpixels. (**A**) The raw (non-normalized) mean rates of change at 64 superpixels across the macular 8 × 8 grid from the Posterior Pole Algorithm of Spectralis SD-OCT for macular outcome measures. (**B**) The standard deviation for the raw rates of change at 64 superpixels across the macular 8 × 8 grid for the same macular outcome measures. FMT, full macular thickness; GCC, ganglion cell complex; GCIPL, ganglion cell/inner plexiform layers; GCL, ganglion cell layer; ORL, outer retinal layers.

coefficient ≥ 0.315 (distance of 0.685 or closer). The detection rates and FDRs for the macular sectors are reported in Table 1. The results were similar to those for superpixels with the FMT displaying the highest detection rates ($P < 0.001$), followed by GCC, ORL, GCIPL, and GCL. The FDR was lowest for FMT ($P < 0.001$) followed by ORL.

Fifteen eyes (13.0%) were determined to be progressing based on PLR criteria. Normalized rates of change as a function of VF progression status are presented in Table 2. Nineteen (17.0%) and 34 (30.4%) eyes progressed according to the alternative PLR and MD criteria, respectively. When all the SPs were included, the rates of change did not significantly differ between progressing and nonprogressing eyes for any of the measures of interest ($P > 0.05$). When only the central 24 superpixels were considered, the rates of change in eyes with perimetric progression were faster than nonprogressing eyes for all the macular measures ($P = 0.01$ for FMT, and $P < 0.001$ for GCC, GCIPL, and GCIPL) except for ORL ($P = 0.88$); differences in structural change rates between eyes with and without perimetric progression were larger in magnitude when only the central 24 superpixels were considered. Detection rates and FDRs for superpixels according to presence or lack of VF progression are

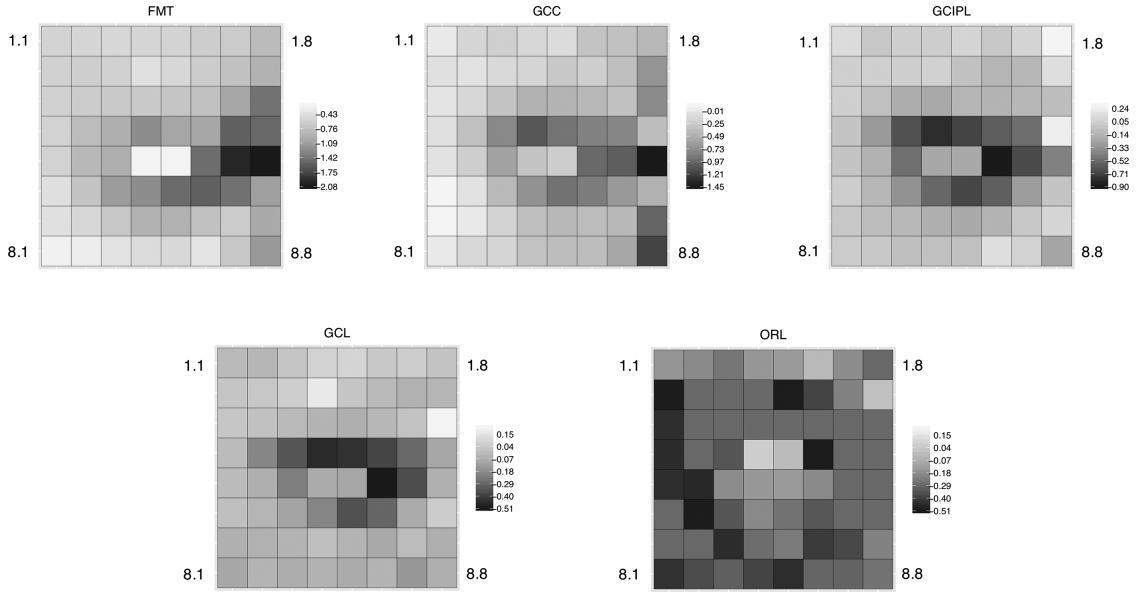

Figure 2. Heat map of the raw rates of change at the 64 superpixels for the various macular outcome measures. Gray-scale representation of raw (non-normalized) rates of change at the 64 superpixels from the Posterior Pole Algorithm of Spectralis SD-OCT for the macular outcome measures explored in the current study. FMT, full macular thickness; GCC, ganglion cell complex; GCIPL, ganglion cell/inner plexiform layers; GCL, ganglion cell layer; ORL, outer retinal layers. Darker shade indicates faster rates of progression.

Table 2. Normalized Rates of Change (Expressed as %/Year) at Macular Superpixels for all Macular Outcome Measures

	Visual Field Status	FMT	GCC	GCIPL	GCL	ORL
All superpixels[a]	Stable	−0.231	−0.275	−0.199	−0.150	−0.205
	Progressing	−0.416	−0.701	−0.317	−0.678	−0.215
	P value	0.11	0.06	0.58	0.06	0.93
Central 24 superpixels	Stable	−0.264	−0.409	−0.357	−0.238	−0.193
	Progressing	−0.552	−1.306	−1.263	−1.467	−0.176
	P value	**0.01**	**<0.001**	**<0.001**	**<0.001**	0.88

FMT, full macular thickness; GCC, ganglion cell complex; GCIPL, ganglion cell/inner plexiform layers; GCL, ganglion cell layer; ORL: outer retinal layers.

Top, all superpixels; bottom, central 24 superpixels.

[a]Excluding the most nasal column of superpixels.

displayed in Table 3. Detection rates were higher in eyes with perimetric progression than in stable eyes for GCC ($P = 0.008$), GCIPL ($P = 0.018$), and GCL ($P < 0.001$), but not for FMT ($P = 0.43$) and ORL ($P = 0.91$). There were no significant differences in FDRs between perimetrically progressing and stable eyes regardless of the macular measure of interest. The subanalyses conducted on the central 24 superpixels yielded similar results. Differences in detection rates between the two groups increased when only the central 24 superpixels were included except for ORL ($P = 0.77$) and FMT ($P = 0.20$) thickness. Conversely, differences in FDRs remained nonsignificant for all the measures of interest. Similar results were obtained when VF progression was based on the MD rate of change; whereas the difference in normalized rates of change, detection rates, and FDRs between perimetrically stable and progressing patients was less evident when using the less restrictive PLR criteria (Supplementary Tables S1, S2).

Baseline thickness measurements of macular outcomes are not directly comparable as they have different average normative values; therefore, we divided the baseline superpixel thickness

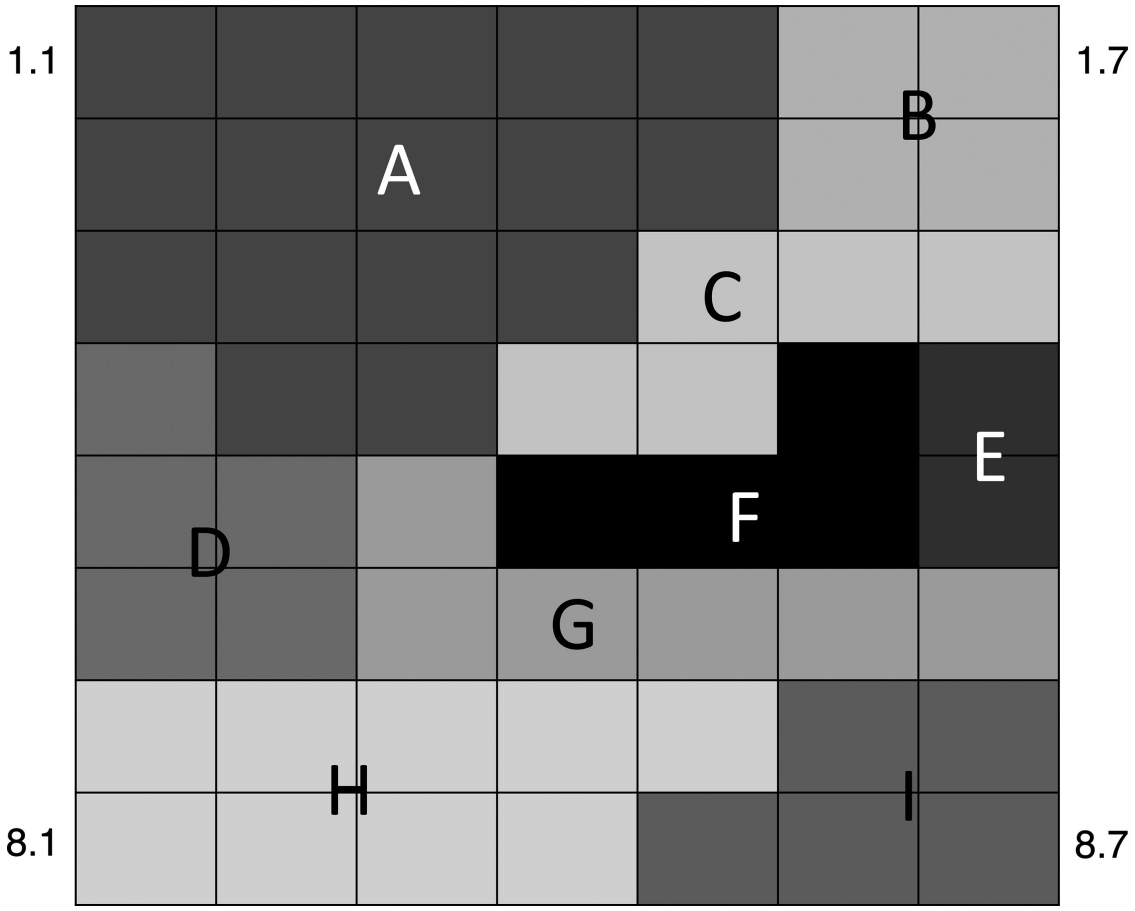

Figure 3. Definition of macular sectors. Macular sectors were defined based on cluster analysis of raw rates of change for full macular thickness, ganglion cell complex, ganglion cell/inner plexiform layers, and ganglion cell layer. A cutoff point of 0.315 for the correlation was used to prune off the resulting dendrogram and create the final 9 macular sectors.

Table 3. Detection Rates and False Discovery Rates at Superpixel Level for Various Macular Measures According to the Visual Field Outcome at the End of Follow-Up

		Detection Rate			False Discovery Rate		
	Macular Measure	VF Stable	VF Progressing	*P* Value	VF Stable	VF Progressing	*P* Value
All superpixels[a]	FMT	25.2%	31.0%	0.43	3.4%	4.2%	0.66
	GCC	13.3%	28.1%	**0.008**	4.0%	7.3%	0.80
	GCIPL	10.3%	19.6%	**0.018**	3.9%	6.9%	0.44
	GCL	6.8%	18.0%	**<0.001**	3.5%	6.8%	0.47
	ORL	14.2%	17.4%	0.91	2.8%	4.3%	0.36
Central 24 superpixels	FMT	27.4%	37.5%	0.20	2.5%	2.2%	0.99
	GCC	18.9%	41.1%	**<0.001**	3.5%	4.4%	0.72
	GCIPL	14.2%	35.0%	**0.001**	3.8%	4.4%	0.89
	GCL	9.5%	30.3%	**<0.001**	3.4%	7.5%	0.23
	ORL	13.6%	15.6%	0.77	3.2%	5.8%	0.33

[a]Superpixels belonging to the most nasal column were excluded. FMT, full macular thickness; GCC, ganglion cell complex; GCIPL, ganglion cell/inner plexiform layers; GCL, ganglion cell layer; ORL, outer retinal layers; VF, visual field.

Detection rate was described as the percentage of superpixels demonstrating a negative slope (rate of change) with a *P* value of < 0.05. Conversely, the false discovery rate was defined as the percentage of superpixels demonstrating a positive slope (rate of change) along with a *P* value < 0.05.

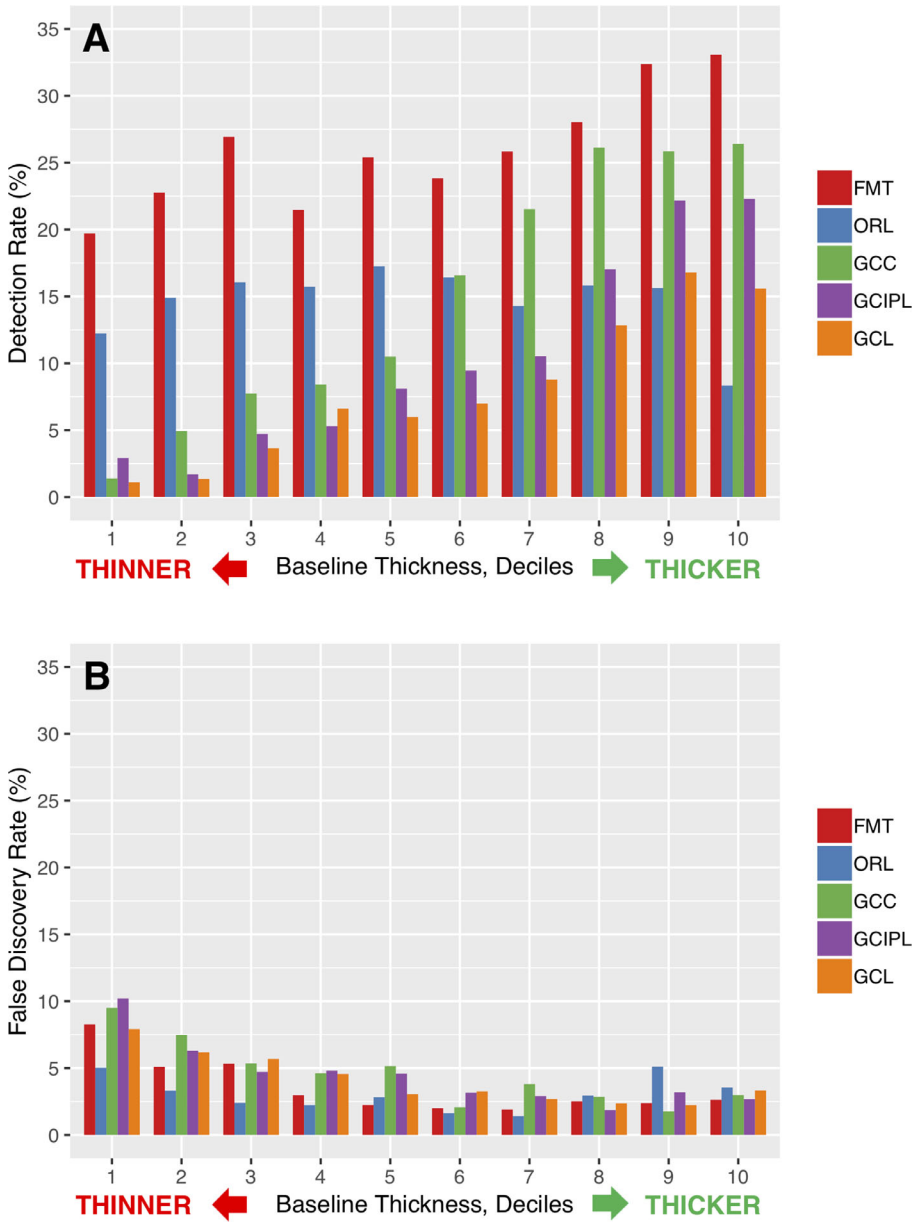

Figure 4. Detection rates and false discovery rates of various macular outcomes stratified for baseline superpixel thickness measurements. The proportion of superpixels demonstrating a negative rate of change (presumed progression: detection rate) (**A**) and positive rate of change (presumed improvement: false discovery rate) (**B**) with *P* value < 0.05 as a function of baseline thickness. The macular thickness at superpixels at baseline for all outcome measures of interest was expressed in deciles to make them comparable. FMT, full macular thickness; GCC, ganglion cell complex; GCIPL, ganglion cell/inner plexiform layers; GCL, ganglion cell layer; ORL, outer retinal layers.

measurements into ten deciles for each measure. Figure 4 shows the proportion of worsening and improving superpixels demonstrating $P < 0.05$ (i.e. detection rates and FDRs) for the five macular measures as a function of baseline thickness. The GCL, GCIPL, and to a lesser extent GCC demonstrated diminishing detection rates with decreasing baseline thickness ($P < 0.001$, Tukey test). This decline was much smaller with FMT ($P < 0.001$, Tukey test) and was not observed with ORL, whose rate of change between deciles 1 to 5 and 6 to 10 did not significantly differ ($P = 0.43$). In addition, FMT detected the highest proportion of worsening superpixels across all macular thickness deciles ($P < 0.01$, Tukey test), except when compared to GCC for the five thickest deciles ($P \geq 0.14$, Tukey test) and to ORL for deciles 2 ($P = 0.26$, Tukey test), 4 ($P = 0.64$, Tukey test), 5 ($P = 0.42$, Tukey test), and 6 ($P = 0.10$, Tukey

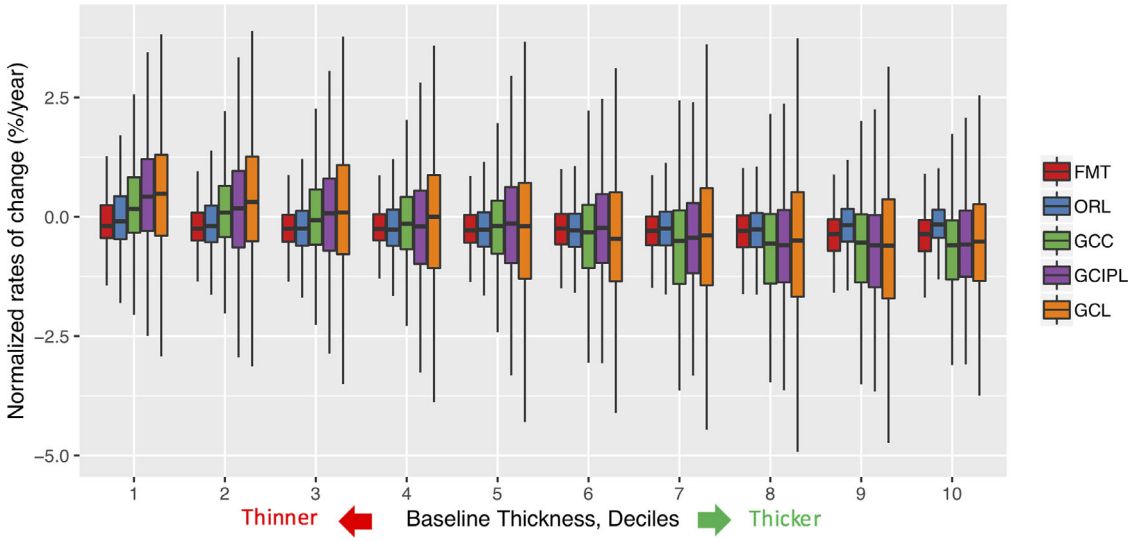

Figure 5. Normalized rates of change of various macular outcomes stratified for baseline superpixel thickness measurements. The boxplot compares normalized rates of change (expressed as percent per year) of superpixels for the five macular outcome measures as a function of the baseline thickness expressed in deciles. FMT, full macular thickness; GCC, ganglion cell complex; GCIPL, ganglion cell/inner plexiform layers; GCL, ganglion cell layer; ORL, outer retinal layers.

test). The FDR was uniformly low for all the macular measures and only slightly increased as the baseline thickness decreased ($P < 0.001$, Tukey test) except for ORL ($P = 0.25$, Tukey test). Figure 5 provides a comparison of macular superpixel rates of change as a function of baseline thickness. Below the third decile, FMT showed faster normalized rates of progression compared to both GCIPL ($P = 0.03$ or below, Tukey test) and GCL ($P < 0.001$, Tukey test), whereas it had significantly faster rates only within the first decile when compared to GCC ($P < 0.001$, Tukey test). On the other hand, FMT rates were significantly slower than GCC for the thickest four deciles ($P = 0.001$ or below, Tukey test). Around the third decile of thickness, the average rates of change for GCC, GCIPL, and GCL reached 0%/year. The variability of rates of change was highest for GCL regardless of baseline thickness. The FMT and ORL normalized rates of change did not significantly differ at any deciles ($P \geq 0.83$, Tukey test).

To further explore the impact of the severity of baseline damage on detection of structural worsening, we stratified the pooled superpixels as a function of their corresponding baseline TD values (Fig. 6). The detection rates decreased with increasing baseline glaucoma damage for GCL, GCIPL, and GCC. Among these three measures, GCC had the highest detection rates along the spectrum of glaucoma severity, and the difference was significant regardless the severity when compared to GCL (Tukey test: $P < 0.001$, $P = 0.004$, and $P = 0.034$ for TD values of > -6, -6 to -12, and < -12 dB, respectively); in contrast, there was no significant difference between GCC and GCIPL along the entire spectrum of 10-2 VF severity ($P \geq 0.38$, Tukey est). There was a significant difference between GCL and GCIPL only in superpixels with the least severe baseline VF damage (Tukey test: $P < 0.001$, $P = 0.25$, and $P = 0.97$ for TD values of > -6, -6 to -12, and < -12 dB, respectively). Among all five macular measures of interest, FMT had the highest detection rate ($P < 0.001$ for all comparisons, except versus ORL at SPs corresponding to VF test locations with moderate [$P = 0.019$] and severe [$P = 0.25$] baseline damage, Tukey test), and its detection rates did not exhibit any significant trend as a function of disease severity. The proportion of superpixels with worsening of ORL increased with glaucoma severity ($P < 0.001$, Tukey test). FDRs were uniformly low for all macular measures, and there was no significant difference within the same macular measure along the entire spectrum of disease severity ($P = 0.08$ or above, Tukey test), except when comparing GCC FDRs for the least and most severe TD severity groups ($P = 0.003$, Tukey test). Figure 7 shows the normalized rates of change of each macular measurement stratified for the baseline TD values. The normalized rates of change for GCL, GCIPL, and GCC became slower (less negative) as the severity of damage increased ($P < 0.001$) and reached 0%/year in locations where the baseline TD was worse than -12 dB. The variability of rates of change was highest for GCL regardless of the baseline TD values. The normalized rates of change of FMT and ORL

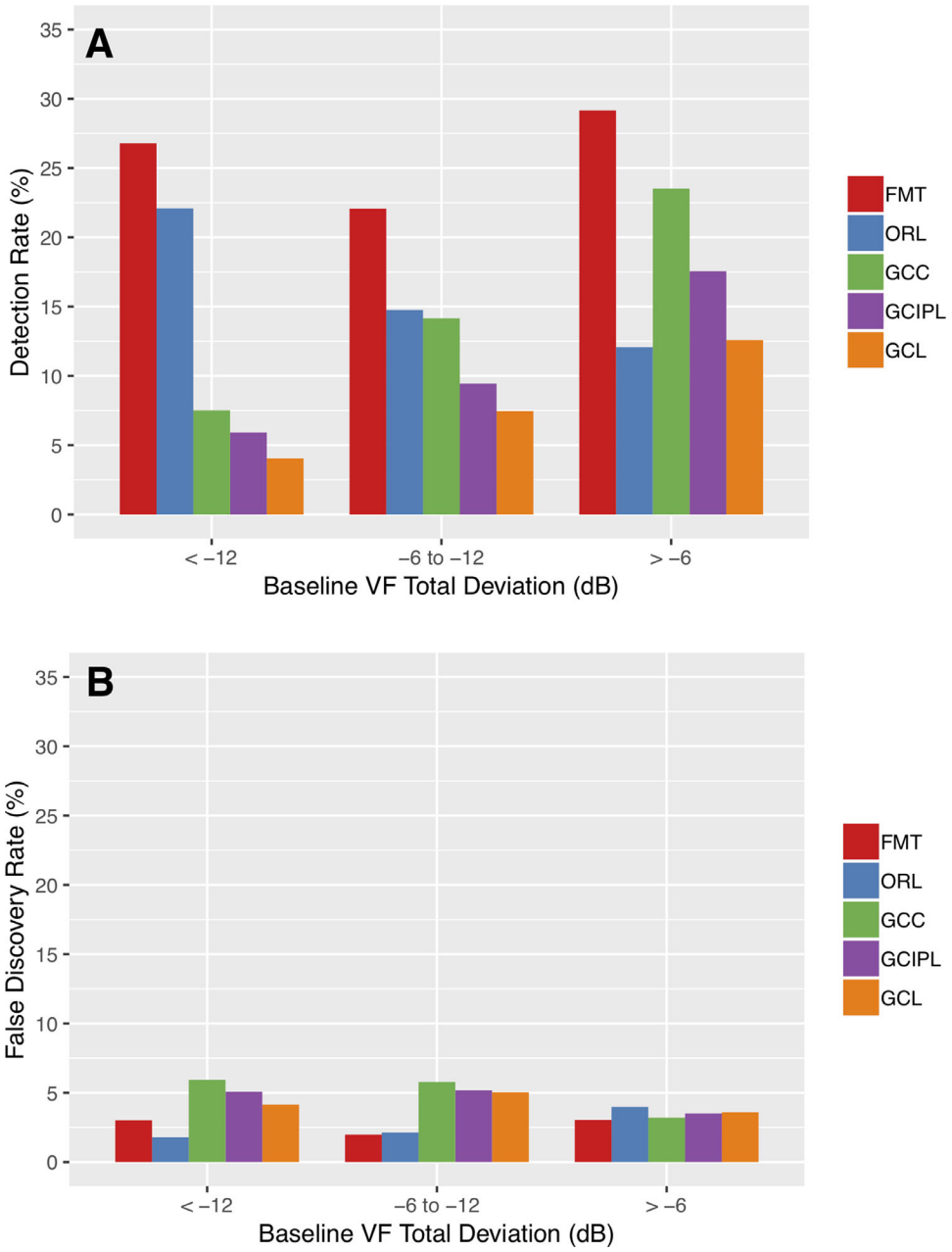

Figure 6. Detection rates and false discovery rates for various macular thickness measures stratified according to baseline total deviation values at 10-2 visual field (VF) locations. The proportion of superpixels demonstrating a negative rate of change (presumed worsening: detection rate) (**A**) and positive rate of change (presumed improvement: false discovery rate) (**B**) with *P* value < 0.05 as a function of baseline 10-2 VF pointwise total deviation. The baseline total deviation values were categorized in three bins according to glaucoma damage at baseline: > -6 dB, between -6 dB and -12 dB, and worse than -12 dB. FMT, full macular thickness; GCC, ganglion cell complex; GCIPL, ganglion cell/inner plexiform layer; GCL, ganglion cell layer; ORL, outer retinal layers.

were similar at the locations with moderate and severe TD damage ($P = 1.0$ and $P = 0.9$, Tukey test), whereas the ORL had significantly slower rates of change for locations with a mild baseline VF damage ($P < 0.001$, Tukey test). The normalized rates of change did not considerably change with disease severity for FMT ($P = 0.99$), whereas they became slightly faster with advancing disease severity for ORL ($P < 0.001$).

Figure 8 provides an UpSet plot for sectoral detection rates according to various macular measures. The highest concordance was observed between FMT and ORL.

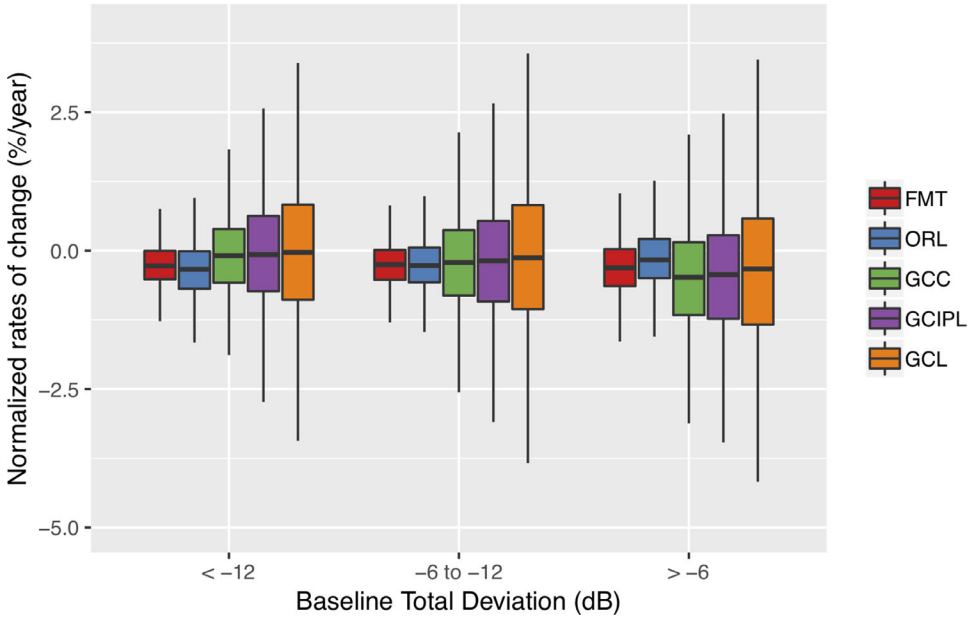

Figure 7. Normalized rates of change of various macular outcomes stratified based on baseline 10-2 visual field (VF) total deviation values. The boxplot compares normalized rates of change at superpixels (expressed as percent per year) for the 5 macular outcomes of interest as a function of baseline 10-2 VF total deviation values. The baseline total deviation values were categorized in three bins (> -6 dB, between -6 dB and -12 dB, and worse than -12 dB). FMT, full macular thickness; GCC, ganglion cell complex; GCIPL, ganglion cell/inner plexiform layer; GCL, ganglion cell layer; ORL, outer retinal layers.

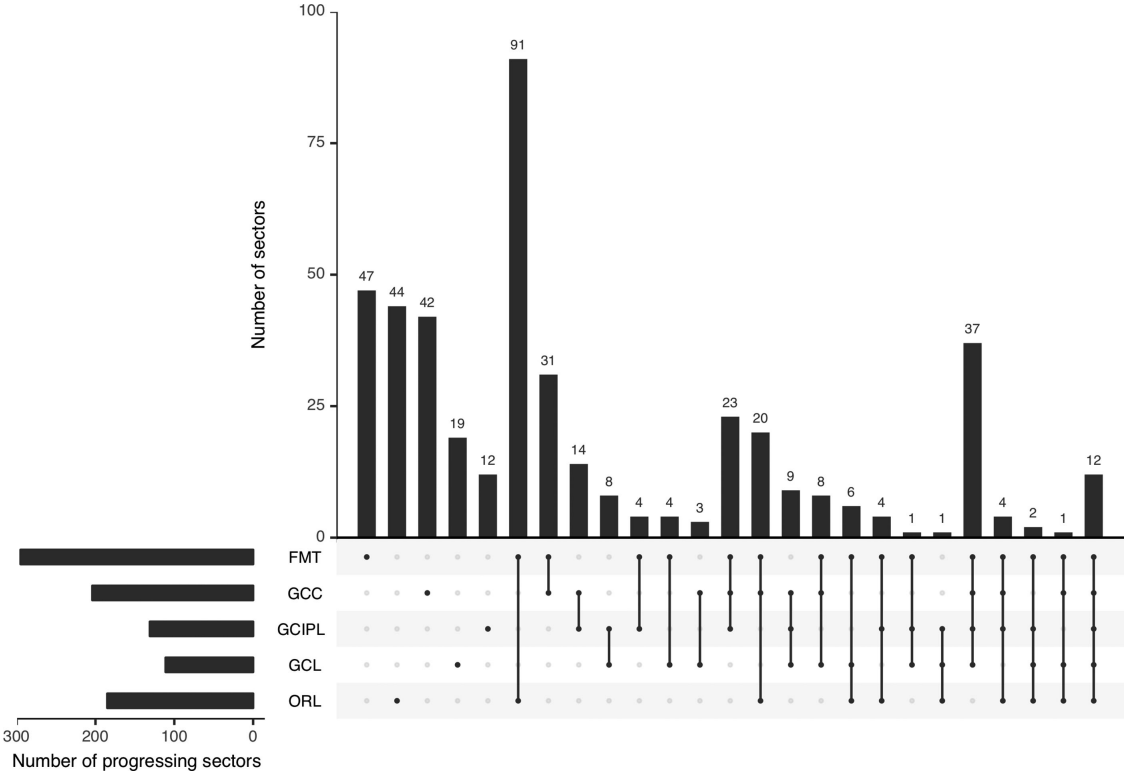

Figure 8. UpSet plot of progressing sectors. UpSet plot of sectors judged as progressing according to each macular measure based on a negative slope with a *P* value of < 0.05. The horizontal histogram (*bottom left*) displays the total number of progressing sectors for each macular measure. The matrix (*bottom*) shows selected measures as *black dots*. When an intersection between two or more measures is displayed, those measures are marked as *black dots* and connected by a *solid black line*. The vertical histogram represents the number of sectors progressing according to a single measure or the intersections between two or more measures. FMT, full macular thickness; GCC, ganglion cell complex; GCIPL, ganglion cell/inner plexiform layers; GCL, ganglion cell layer; ORL, outer retinal layers.

Discussion

Macular OCT imaging has become an accepted approach to detect early glaucoma and provides information about retinal ganglion cells (RGCs) in the central retina. Macular RGCs relay central visual information to the brain and are functionally the most crucial among RGCs. With improved resolution of OCT devices, measurement of individual inner retinal layers including GCL is now clinically possible although none of the studies comparing GCL thickness to other measures have demonstrated its superiority for detecting early glaucoma damage.[10,24,25]

Detection of disease progression is affected by the reproducibility of the outcome measure used. Reproducibility of global, sectoral, and local macular measurements has been demonstrated to be high.[26–28] Miraftabi et al.[12] recently showed that regardless of the outcome measured (including FMT, GCC, GCIPL, and GCL), intra-session variability at superpixels is low and uniform across the macula. With advancing glaucoma and decreased inner layer thickness measurements, GCL and GCIPL measurement's variability increases as they approach their measurement floor.[12] We hypothesized that measuring thicker slabs of macular tissue (GCC or FMT) would pose a less challenging segmentation task and result in less noisy measurements as glaucoma worsens to advanced stages and, therefore, such measures would perform better for detection of change compared to GCL or GCIPL.

We found that FMT measurements were more likely to detect statistically significant trends at superpixels or sectors over time, followed by GCC measurements. This was despite similar FDRs for all macular measures. However, the ORL rates also showed a similar trend. Two findings suggest that ORL's downward trends represent possible aging effect rather than glaucoma worsening. First, the distribution of superpixel rates of change was mostly diffuse and did not follow the pattern seen with other macular measures (see Fig. 2). In addition, rates of ORL change were not different in perimetrically progressing eyes compared to stable ones. This is consistent with conclusions of previous studies that ORLs are not affected by glaucoma and that ORL thickness decreases with age rather than disease severity.[16,17,29]

Due to the relatively short-term follow-up, the overall magnitude of trends was small, and we did not expect to detect large changes in the central VF. The average worsening of MD on the 10-2 fields was about 1 dB in the entire group over the course of the follow-up. The variability of macular rates of change decreased with increasing thickness. Normalized FMT rates demonstrated lower variability and tended to be larger. Given our approach for normalization, normalized FMT rates would be expected to be slower than GCC rates as tissue thinning in glaucoma occurs in the inner retina. FMT rates of change are partially driven by ORL change rates, which likely represent age-related decay. Although there is no evidence that the outer retina is affected in glaucoma,[16] age-related changes do occur in the outer retina, which could explain the faster FMT rates of change compared to GCC.[19,29] This is also supported by the fact that FMT and ORL showed the highest agreement on the UpSet plot (see Fig. 8).

Correlation of adjacent VF test locations or neighboring superpixels in the macula is a well-known issue with regard to detection of change. We addressed this issue in two different ways. First, we used mixed models with the eye considered as a random effect to account for within-eye correlations. Second, we grouped superpixels into distinct macular sectors based on partial correlations of raw rates of change adjusted for the pooled normative thickness of each pair of SPs. The remaining correlation between sectors was small and unlikely to be of clinical significance since we used a lenient cutoff of 0.315 for clustering of rates of change. The results of sectoral analyses were similar to and corroborated those for superpixels.

The faster rates of change detected by FMT and GCC may be confounded by aging effects. The FMT or GCC had the highest ability for detection of thickness changes over time regardless of the underlying mechanism; at least some of the detected change likely represents real progression. We compared rates of change in eyes progressing based on pointwise linear regression of 10-2 VF series to stable eyes. When all SPs were included in the comparison, the difference in structural rates of change were not different between perimetrically progressing and stable; when the analyses were repeated including only the central 24 superpixels, all macular outcome measures except ORL displayed faster rates of progression in functionally deteriorating eyes. The central 24 superpixels sample the central 18° of the macula where the bulk of macular RGCs are located and where stronger structure-function relationships are observed.[10] This further confirms the validity of our findings. In addition, GCC detection rates were higher compared to GCIPL and GCL at comparable FDR in the central macula. Normalized GCC rates of change were also equal or lower (more negative) regardless of the baseline thickness or 10-2 VF total deviation values at corresponding test locations compared to GCIPL and GCL. These two findings imply that GCC may be the optimal outcome measure to be used

for detection of glaucoma progression regardless of disease severity.

One limitation of our study is the lack of a normal control group so that the specificity of our progression criteria could be formally compared. Aging-related rates of change have been reported to vary between −0.10 and −0.5 µm/year for GCC and GCIPL.[30–35] The fact that functionally progressing eyes demonstrated a higher proportion of worsening superpixels validates the notion that the observed rates of change at least partially reflect real disease deterioration. The follow-up length was fairly short in this cohort and, therefore, age-related decay would be expected to be small. We continue to monitor this cohort and will be revisiting this issue after the study eyes have been followed for a minimum of 5 years.

In summary, our findings strongly suggest that GCC thickness measurements are likely the optimal macular outcome measure for detection of glaucoma deterioration in patients along the spectrum of disease severity. Increasing measurement noise with advancing glaucoma diminishes the efficiency of macular measures for detection of change. Relying on FMT measures may lead to an overdiagnosis of progression.

Acknowledgments

The authors thank Jeff Gornbein, DrPH, Department of Biomathematics, David Geffen School of Medicine, UCLA, for statistical expertise and assistance.

Supported by NIH R01EY029792 (K.N.M.), Departmental grant from Research to Prevent Blindness (K.N.M.), Heidelberg Engineering (K.N.M.).

Presented as an oral paper at the annual meeting of the Association for Research in Vision and Ophthalmology, Honolulu, HI, USA, May 2018.

Disclosure: **A. Rabiolo,** Santen Italy srl; **V. Mohammadzadeh,** None; **N. Fatehi,** None; **E. Morales,** None; **A.L. Coleman,** None; **S.K. Law,** None; **J. Caprioli,** Aerie, Alcon, Allergan, Glaukos, New World Medical; **K. Nouri-Mahdavi,** Heidelberg Engineering, Aerie

References

1. de Moraes CG, Liebmann JM, Medeiros FA, Weinreb RN. Management of advanced glaucoma: characterization and monitoring. *Surv Ophthalmol*. 2016;61:597–615.
2. Russell RA, Crabb DP, Malik R, Garway-Heath DF. The relationship between variability and sensitivity in large-scale longitudinal visual field data. *Invest Ophthalmol Vis Sci*. 2012;53:5985–5990.
3. De Moraes CG, Liebmann JM, Park SC, et al. Optic disc progression and rates of visual field change in treated glaucoma. *Acta Ophthalmol*. 2013;91:e86–e91.
4. Jampel HD, Friedman D, Quigley H, et al. Agreement among glaucoma specialists in assessing progressive disc changes from photographs in open-angle glaucoma patients. *Am J Ophthalmol*. 2009;147:39–44.e31.
5. Mwanza JC, Budenz DL, Warren JL, et al. Retinal nerve fibre layer thickness floor and corresponding functional loss in glaucoma. *Br J Ophthalmol*. 2015;99:732–737.
6. Hood DC, Anderson SC, Wall M, Kardon RH. Structure versus function in glaucoma: an application of a linear model. *Invest Ophthalmol Vis Sci*. 2007;48:3662–3668.
7. Shin JW, Sung KR, Lee GC, Durbin MK, Cheng D. Ganglion cell-inner plexiform layer change detected by optical coherence tomography indicates progression in advanced glaucoma. *Ophthalmology*. 2017;124:1466–1474.
8. Belghith A, Medeiros FA, Bowd C, et al. Structural change can be detected in advanced-glaucoma eyes. *Invest Ophthalmol Vis Sci*. 2016;57:Oct511–518.
9. Lavinsky F, Wu M, Schuman JS, et al. Can macula and optic nerve head parameters detect glaucoma progression in eyes with advanced circumpapillary retinal nerve fiber layer damage? *Ophthalmology*. 2018;125:1907–1912.
10. Miraftabi A, Amini N, Morales E, et al. Macular SD-OCT outcome measures: comparison of local structure-function relationships and dynamic range. *Invest Ophthalmol Vis Sci*. 2016;57:4815–4823.
11. Chien JL, Ghassibi MP, Patthanathamrongkasem T, et al. Glaucoma diagnostic capability of global and regional measurements of isolated ganglion cell layer and inner plexiform layer. *J Glaucoma*. 2017;26:208–215.
12. Miraftabi A, Amini N, Gornbein J, et al. Local variability of macular thickness measurements with SD-OCT and influencing factors. *Transl Vis Sci Technol*. 2016;5:5.
13. Liu Y, Simavli H, Que CJ, et al. Patient characteristics associated with artifacts in Spectralis optical coherence tomography imaging of the retinal nerve fiber layer in glaucoma. *Am J Ophthalmol*. 2015;159:565–576.e562.

14. Mansberger SL, Menda SA, Fortune BA, Gardiner SK, Demirel S. Automated segmentation errors when using optical coherence tomography to measure retinal nerve fiber layer thickness in glaucoma. *Am J Ophthalmol*. 2017;174:1–8.
15. Pazos M, Dyrda AA, Biarnes M, et al. Diagnostic accuracy of Spectralis SD OCT automated macular layers segmentation to discriminate normal from early glaucomatous eyes. *Ophthalmology*. 2017;124:1218–1228.
16. Vianna JR, Butty Z, Torres LA, et al. Outer retinal layer thickness in patients with glaucoma with horizontal hemifield visual field defects. *Br J Ophthalmol*. 2019;103:1217–1222.
17. Cifuentes-Canorea P, Ruiz-Medrano J, Gutierrez-Bonet R, et al. Analysis of inner and outer retinal layers using spectral domain optical coherence tomography automated segmentation software in ocular hypertensive and glaucoma patients. *PLoS One*. 2018;13:e0196112.
18. Na JH, Sung KR, Baek S, et al. Detection of glaucoma progression by assessment of segmented macular thickness data obtained using spectral domain optical coherence tomography. *Invest Ophthalmol Vis Sci*. 2012;53:3817–3826.
19. Nieves-Moreno M, Martínez-de-la-Casa JM, Morales-Fernández L, Sánchez-Jean R, Sáenz-Francés F, García-Feijoó J. Impacts of age and sex on retinal layer thicknesses measured by spectral domain optical coherence tomography with Spectralis. *PLoS One*. 2018;13:e0194169.
20. Rabiolo A, Morales E, Mohamed L, et al. Comparison of methods to detect and measure glaucomatous visual field progression. *Transl Vis Sci Technol*. 2019;8:2.
21. de Moraes CG, Song C, Liebmann JM, Simonson JL, Furlanetto RL, Ritch R. Defining 10-2 visual field progression criteria: exploratory and confirmatory factor analysis using pointwise linear regression. *Ophthalmology*. 2014;121:741–749.
22. Drasdo N, Millican CL, Katholi CR, Curcio CA. The length of Henle fibers in the human retina and a model of ganglion receptive field density in the visual field. *Vision Res*. 2007;47:2901–2911.
23. Raza AS, Cho J, de Moraes CG, et al. Retinal ganglion cell layer thickness and local visual field sensitivity in glaucoma. *Arch Ophthalmol*. 2011;129:1529–1536.
24. Michelessi M, Riva I, Martini E, et al. Macular versus nerve fibre layer versus optic nerve head imaging for diagnosing glaucoma at different stages of the disease: Multicenter Italian Glaucoma Imaging Study. *Acta Ophthalmol*. 2019;97:e207–e215.
25. Elbendary AM, Abd El-Latef MH, Elsorogy HI, Enaam KM. Diagnostic accuracy of ganglion cell complex substructures in different stages of primary open-angle glaucoma. *Can J Ophthalmol*. 2017;52:355–360.
26. Kim KE, Yoo BW, Jeoung JW, Park KH. Long-term reproducibility of macular ganglion cell analysis in clinically stable glaucoma patients. *Invest Ophthalmol Vis Sci*. 2015;56:4857–4864.
27. Francoz M, Fenolland JR, Giraud JM, et al. Reproducibility of macular ganglion cell-inner plexiform layer thickness measurement with cirrus HD-OCT in normal, hypertensive and glaucomatous eyes. *Br J Ophthalmol*. 2014;98:322–328.
28. Lee MW, Park KS, Lim HB, Jo YJ, Kim JY. Long-term reproducibility of GC-IPL thickness measurements using spectral domain optical coherence tomography in eyes with high myopia. *Sci Rep*. 2018;8:11037.
29. Xu Q, Li Y, Cheng Y, Qu Y. Assessment of the effect of age on macular layer thickness in a healthy Chinese cohort using spectral-domain optical coherence tomography. *BMC Ophthalmol*. 2018;18:169.
30. Zhang X, Francis BA, Dastiridou A, et al. Longitudinal and cross-sectional analyses of age effects on retinal nerve fiber layer and ganglion cell complex thickness by fourier-domain OCT. *Transl Vis Sci Technol*. 2016;5:1.
31. Demirkaya N, van Dijk HW, van Schuppen SM, et al. Effect of age on individual retinal layer thickness in normal eyes as measured with spectral-domain optical coherence tomography. *Invest Ophthalmol Vis Sci*. 2013;54:4934–4940.
32. Kim NR, Kim JH, Lee J, Lee ES, Seong GJ, Kim CY. Determinants of perimacular inner retinal layer thickness in normal eyes measured by Fourier-domain optical coherence tomography. *Invest Ophthalmol Vis Sci*. 2011;52:3413–3418.
33. Girkin CA, McGwin G, Jr., Sinai MJ, et al. Variation in optic nerve and macular structure with age and race with spectral-domain optical coherence tomography. *Ophthalmology*. 2011;118:2403–2408.
34. Ueda K, Kanamori A, Akashi A, Tomioka M, Kawaka Y, Nakamura M. Effects of axial length and age on circumpapillary retinal nerve fiber layer and inner macular parameters measured by 3 types of SD-OCT instruments. *J Glaucoma*. 2016;25:383–389.
35. Leung CK, Ye C, Weinreb RN, Yu M, Lai G, Lam DS. Impact of age-related change of retinal nerve fiber layer and macular thicknesses on evaluation of glaucoma progression. *Ophthalmology*. 2013;120:2485–2492.